ACS OMEGA

http://pubs.acs.org/journal/acsodf

Article

Impact of Individual Cell Parameter Difference on the Performance of Series−Parallel Battery Packs

Yongqi Wang, Yujie Zhao, Siyuan Zhou, Qingzhong Yan, Han Zhan, Yong Cheng,* and Wei Yin*

Cite This: *ACS Omega* 2023, 8, 10512−10524

Read Online

ACCESS | Metrics & More | Article Recommendations

ABSTRACT: Lithium-ion power batteries are used in groups of series−parallel configurations. There are Ohmic resistance discrepancies, capacity disparities, and polarization differences between individual cells during discharge, preventing a single cell from reaching the lower limit of the terminal voltage simultaneously, resulting in low capacity and energy utilization. The effect of the parameter difference (difference in parameters) of individual cells on the performance of the series−parallel battery pack is simulated and analyzed by grouping cells with different parameters. The findings reveal that when cells are connected in series, the capacity difference is a significant factor impacting the battery pack's energy index, and the capacity difference and Ohmic resistance difference are significant variables affecting the battery pack's power index. When cells are connected in parallel, the difference in Ohmic internal resistance between them causes branch current imbalance, low energy utilization in some individual cells, and a sharp expansion of unbalanced current at the end of discharge, which is prone to overdischarge and shortens battery life. Interestingly, we found that when there is an aging cell in a series−parallel battery pack, the terminal voltage of the single battery module containing the aging single cell will decrease sharply at the end of discharge. Evaluating the change rate of battery module terminal voltage at the end of discharge can be used as a method to evaluate the aging degree of the battery module. The research results provide a reference for connecting batteries to battery packs, particularly the screening of retired power battery packs and the way to reconnect into battery packs.

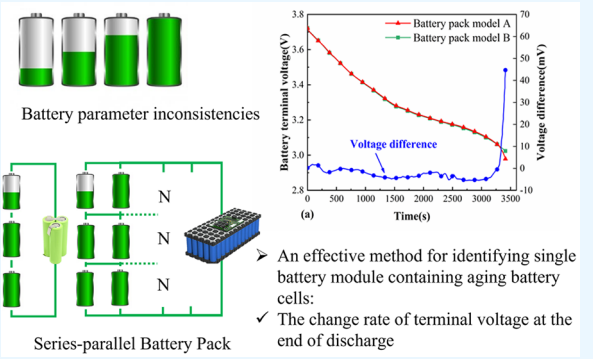

1. INTRODUCTION

With the aggravation of environmental pollution, people are paying more and more attention to the application of clean energy under the urgent need for energy conservation and carbon reduction.[1−5] Because of its advantages of high energy density, high power, long cycle life, little self-discharge, and green environmental protection, lithium-ion batteries are extensively employed in civil industries such as electric cars and energy storage.[6] On the other hand, the voltage and capacity of an individual cell cannot fulfill the criteria and characteristics of the electric vehicle's power system. To achieve the vehicle's real performance needs, multiple cells must be connected in series/parallel.[7,8]

The parameter difference of cells mainly comes from the manufacturing or storage process and the use process.[9,10] The battery parameter difference in the manufacturing process is frequently decreased indirectly by controlling the precision of the manufacturing process, but this can only lower the initial parameter difference and cannot be removed. The battery's parameter difference is transferred cumulatively and is affected by the interaction of many factors, and the subtle differences in the initial parameters during use will be infinitely amplified. There will be some differences between the cells in the power battery pack, and as the number of individual cells increases, the problem of battery parameter difference is particularly prominent. The problem of the difference in performance parameters of the cells will cause a series of problems such as shortened battery life, battery pack performance, and safety. The battery parameter difference has become a key factor in the development of power batteries.[11,12] Welding resistance can aggravate cell-to-cell variations when cells are joined in a pack busbar. During the working period of the battery pack, these variables create nonuniform current, voltage, temperature, and battery characteristics, which can lead to battery pack aging.[13] The parameter difference of the battery pack is caused due to the complex charging and discharging environment, temperature, and other external factors in the process of use, combined with differences in the capacity, internal resistance, and self-discharge rate of the individual cells in the manufacturing process. As the battery pack deteriorates,

Received: January 14, 2023
Accepted: February 24, 2023
Published: March 6, 2023

the "barrel effect" of the battery pack steadily expands, limiting the battery pack's available capacity, shortening its service life, and potentially triggering safety problems.[14,15] As a result, various researchers have developed screening techniques for choosing and grouping homogeneous cells.[16,17]

The screening method is mainly based on voltage, resistance, capacity, and other parameters to identify inconsistency in the battery pack, which is divided into signal processing, model, and data fusion methods. The signal processing method is to collect the time-domain voltage and current data in the laboratory to identify the encapsulation parameter difference of lithium batteries.[18,19] The model-based technique predicts the resistance and capacity of a single cell in a charge−discharge experiment using an adaptive filter to match the equivalent circuit model with the observed data.[20,21] The data fusion approach employs mathematical theories such as information entropy,[22] principal component analysis,[23] and copula theory[24] to directly measure the parameter difference of a single cell. These approaches are used to choose the cell before it is used in groups to minimize the initial variation between the individual cells. However, there have been few types of research on the impact of differences in the basic characteristics of a single cell on capacity utilization and energy utilization when the battery pack is in series−parallel groups.

Many scholars have contributed to the modeling of lithium batteries by developing mathematical models, electrochemical models, and equivalent circuit models based on different research objects and mechanisms.[25−27] The mathematical model is generally abstracted from the actual object, and the internal relationship of the object is represented by a mathematical equation. At present, ANNs (artificial neural networks) are routinely utilized to model the battery's exterior features. Without studying the intricate electrochemical changes inside the battery, an artificial neural network bionic human thinking mode is established by gathering a large amount of data for reasoning and then establishing the input and output connection based on the nonlinear benefits of data. The electrochemical model is mainly used to reflect the battery's internal reaction process. It is required to connect the internal status of the battery with the basic process of energy creation of the battery by analyzing macroscopic data outside the battery (such as voltage and current) and internal microscopic particle activities (ion concentration distribution, transmission, etc.).[28] However, because the electrochemical model is too complicated to calculate, it is rarely used to design an electric vehicle's power battery pack.[29] Unlike the electrochemical and mathematical models, the equivalent circuit model of the battery is generally made up of common circuit components such as resistance, capacitance, inductance, and voltage source, and it can accurately replicate the battery's dynamic properties. Rint, Thevenin, PNGV, and GNL are some of the most common equivalent circuit models.[30,31] Idaho State Laboratory proposed the Rint model, but it is incapable of simulating the battery's dynamic characteristics, such as polarization resistance variation. The Thevenin model is a typical nonlinear model, which can properly describe the dynamic process of battery operation. It has a simple structure, easy parameter identification, and convenient expansion of various parameters. However, most battery modeling research in the world focuses on the basic equivalent model of individual cells, and internal battery parameter difference has rarely been explored in group and system models.[32,33]

In this paper, MATLAB-Simulink is used to build the Thevenin model of a series−parallel battery module, and the model's correctness is subsequently verified by experiments. The real capacity utilization and energy utilization of the series-connected battery pack under the Ohmic resistance difference, capacity difference, and polarization difference of the series-connected battery pack are simulated and studied using the battery pack simulation model. The effect of Ohmic resistance differential on the current and SOC (state of charge) of the parallel-connected battery pack, as well as the effect of an aging cell on series−parallel battery pack performance, are investigated. The group optimization idea of a series−parallel single cell is suggested based on the aforementioned simulation.

2. ESTABLISHMENT AND VERIFICATION OF BATTERY PACK MODEL

2.1. Basic Principle of Battery Model. Many scholars have studied the construction of the battery model. Among them, the battery modeling method based on the equivalent circuit model is widely used. The common equivalent circuit models mainly include the Rint model, the Thevenin model, and the PNGV model. The research content of this paper does not involve the exploration of the electrochemical mechanism of the battery and does not need to consider the complex changes in the battery microstructure. The focus is on the external characteristics of the physical quantities such as the terminal voltage and current of the battery. Therefore, compared with the second-order RC equivalent circuit model, the first-order RC requires only a small amount of calculation and the accuracy can solve most engineering application problems. This paper adopts the first-order RC equivalent circuit model.

The Thevenin equivalent circuit model of a single cell is shown in Figure 1. U_{OCV} is the battery's open-circuit voltage,

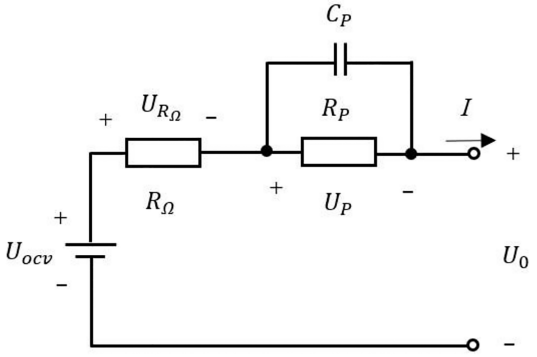

Figure 1. Thevenin equivalent circuit model of a single cell.

R_Ω is the battery's Ohmic internal resistance, I is the battery's current, C_p is the polarization capacitance, R_p is the polarization internal resistance, U_p is the polarization voltage, and R_Ω, C_p, R_p, and other parameters are related to the battery's SOC, temperature, and aging degree, among many other things.

The battery's terminal voltage by an electric circuit dynamic analysis can be expressed as[34]

$$V = U_{OCV} - U_R - IR_p(1 - e^{-t/R_pC_p}) \quad (1)$$

https://doi.org/10.1021/acsomega.3c00266
ACS Omega 2023, 8, 10512−10524

The parameters that the single-cell Thevenin model requires to identify in advance are U_{OCV}, R_Ω, R_p, and C_p.

2.2. Parameter Identification of Battery Model.

2.2.1. Battery and Experimental Equipment. In this paper, the ternary lithium-ion battery produced by China Tianjin Qinxin New Energy Research Institute is used. The main technical parameters of the single cell that was tested are shown in Table 1.

Table 1. Main Technical Parameters of the Single Cell That Was Tested

parameter	value
material	ternary lithium-ion battery
size	diameter 18 mm, height 65 mm
quality	44 g
nominal capacity	2 Ah
nominal voltage	3.7 V
cutoff voltage	charge: 4.2 V
	discharge: 2.75 V
operating temperature range	charge: 0−60 °C
	discharge: −20 to 60 °C
highest continuous current	5C
internal resistance	≤20 mΩ

The experimental platform includes the power battery performance test platform, high-precision data acquisition equipment, programmable temperature cycle test box, computer, etc. The main technical parameters of related test equipment are shown in Table 2. During the charging and discharging operation of the single cell, the high-precision data acquisition equipment collects the information on the terminal voltage, current, power, and other information on the cell in real time and then sends and stores the data to the computer.

Table 2. Main Technical Parameters of Related Test Equipment

equipment	pattern	value
programmable temperature cycle test box	Y70-1-DZ	operating temperature range: −60 to 150 °C (±0.1 °C)
		operating temperature fluctuation: ≤±0.5 °C
		operating temperature resolution: 0.01 °C
power battery performance test platform A	S08-5-100-DZ	operating voltage range: 0−5 V (0.1%FS)
		operating current range: 500 mA to ∼100 A (0.1% FS)
power battery performance test platform B	BTS550C8	operating voltage range: 0−5 V (0.1%FS)
		operating current range: 150 mA to 50 A (0.1% FS)
high-precision data acquisition equipment	ART-USB8812	number of channels: 4
		resolution: 24 bit
		input voltage range: ±11 V, ±5.5 V
		sampling method: synchronous acquisition
		sampling frequency: 8 Hz to 216 kHz
		input impedance: 1 MΩ

The programmable temperature cycle test box controls the ambient temperature at which the cell operates.

2.2.2. Battery SOC Calculation and Capacity Correction. The ampere-hour integration technique is used to calculate the battery's state of charge (SOC), and the formula is as follows:

$$\mathrm{SOC}_{(k+1)} = \mathrm{SOC}_{(k)} + \frac{\eta T}{C} I_k \tag{2}$$

In the formula, $\mathrm{SOC}_{(k)}$ indicates the state of charge of the single battery at time k, I_k represents the working current of the single battery at time k, and when I_k is positive, it signifies charging, and when it is negative, it signifies discharging. C is the rated capacity of the battery, η is the battery's charge and discharge efficiency, and T is the discrete time.

The available capacity of a battery is affected by the temperature, discharge rate, and cycle times. The available capacity of battery is more sensitive to the temperature and discharge rate. Two 18650 cells C and D were selected, and the constant current discharge technique was used to assess the batteries' available capacity at different batteries' discharge rates. The batteries' discharge rates are set to 0.1, 0.5, 1, 3, and 5C. C_a−I_r relationship curve test steps are shown in Figure 2a. Two 18650 cells C and D were selected and discharged to the batteries' cutoff voltage at 0.5 C. The batteries' temperature is adjusted to −20, −Z, 10, 40, and 55 °C, and the test steps ares shown in Figure 2b. C_a is the battery's available capacity, I_r is the battery's discharge rate, and T is the battery's temperature.

Figure 3a shows that as the battery's discharge rate increases, the battery's available capacity decreases. However, for the cell we selected and tested, the discharge rate of the battery has little effect on the available capacity of the battery. Even if the battery capacity is not corrected during experiments with different battery discharge rates, the calculation error is within an acceptable range.

Figure 3b shows that the ambient temperature has a significant impact on the battery's available capacity, with the impact of low temperature on the battery capacity being particularly pronounced. When the ambient temperature falls below 10 °C, the slope of the battery capacity reduction accelerates. The electrical conductivity of the electrodes, separators, electrolytes, and other components inside the battery is severely influenced in a low-temperature environment, causing the battery's performance to rapidly degrade. Furthermore, at low temperatures, the battery's interior materials may accelerate aging and may potentially produce battery safety issues. As a result, utilizing the battery at low temperatures necessitates preheating. The usable capacity of the battery at high temperatures is increased to some extent in comparison to that at low temperatures, primarily because the higher temperature increases chemical activity inside the battery. However, the battery has a safety hazard in a high-temperature environment, because the high-temperature environment will destroy the chemical balance in the battery and cause side reactions.[35] The battery's health will be jeopardized if adverse responses occur. A thermal runaway will occur inside the battery if the temperature rises too high, causing the risk of a battery explosion.

2.2.3. Battery Open-Circuit Voltage Identification. The OCV (open circuit voltage) and SOC (state of charge) curves were estimated by an HPPC (hybrid pulse power characterization) experiment. The HPPC experiment adopts the method of repeatedly discharging the cell at a 0.5C rate until the cell's cutoff voltage is reached, and there is a polarization

https://doi.org/10.1021/acsomega.3c00266
ACS Omega 2023, 8, 10512−10524

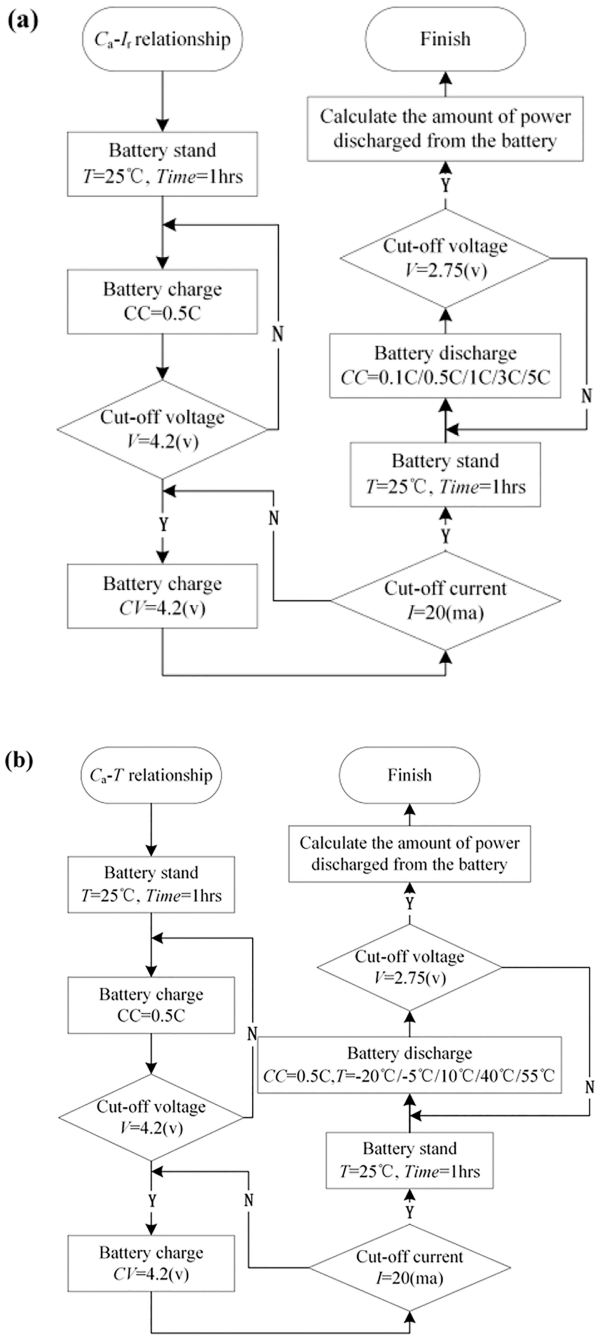

Figure 2. (a) C_a–I_r and (b) C_a–T relationship curve test steps.

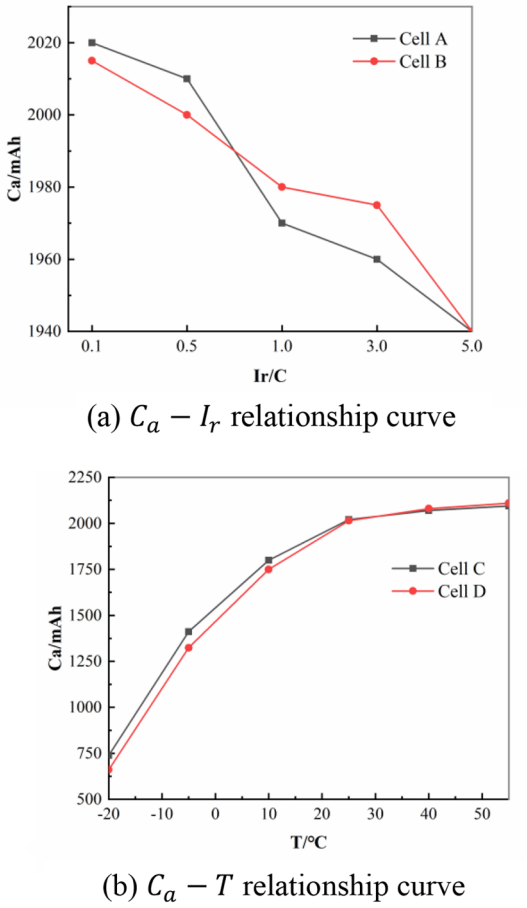

Figure 3. (a) C_a–I_r and (b) C_a–T relationship curves.

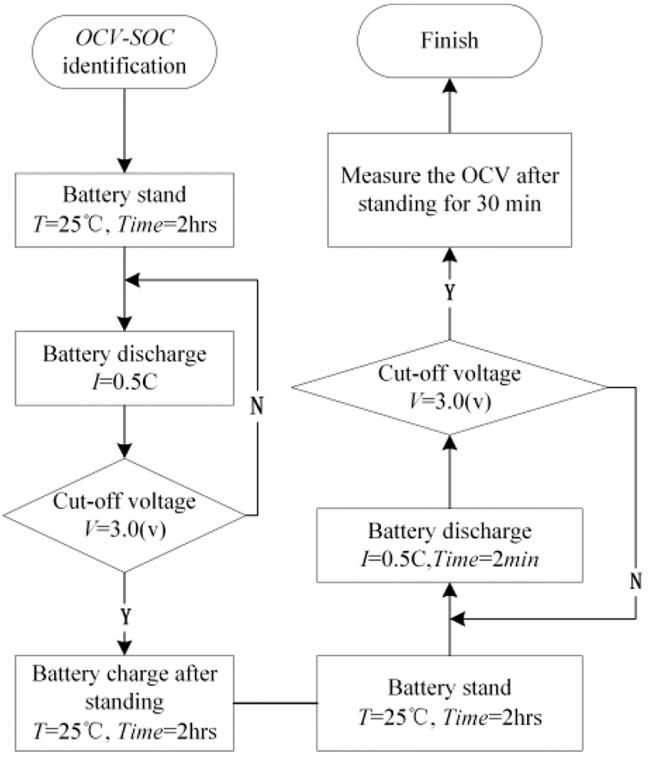

Figure 4. HPPC experimental flowchart.

effect in the single cell. At the end of the discharge, the cell's terminal voltage is not equal to the cell's OCV, and the polarization effect can be eliminated by keeping the stationary state. The HPPC experimental procedure is shown in Figure 4 using a flowchart.

A polynomial fitting was performed on the OCV and SOC curves obtained by the HPPC experiment. The OCV fitting diagram of the single cell is shown in Figure 5. The R^2 value was 0.9973, and the RMSE was 0.00188, both of which satisfy the 95% confidence interval requirements. The fitting curve is estimated as

https://doi.org/10.1021/acsomega.3c00266
ACS Omega 2023, 8, 10512−10524

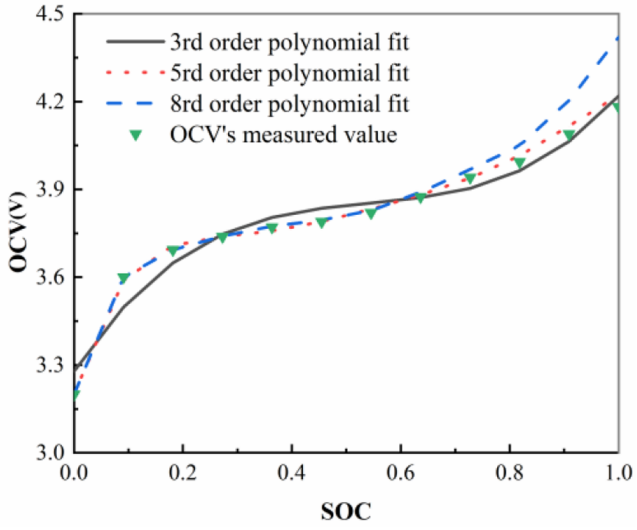

Figure 5. OCV fitting diagram of the single-cell battery.

$$f(x) = 13.958x^5 - 41.693x^4 + 47.098x^3 - 24.259x^2 + 5.874x + 3.208 \quad (3)$$

where x is the SOC value of the single cell and $f(x)$ is the OCV value of the single cell.

2.2.4. Battery Ohmic Internal Resistance and RC Parameter Identification. In this study, the HPPC experiment is carried out utilizing a 2 Ah ternary lithium battery as the test item. The parameter identification is performed every 10% of the battery's SOC points, yielding a total of 11 R_0, R_p, and C_p values of the battery's SOC points, as shown in Figure 6. The battery parameter values at any point in the battery's SOC range of 0−100% are determined via linear interpolation of two consecutive battery SOC points.

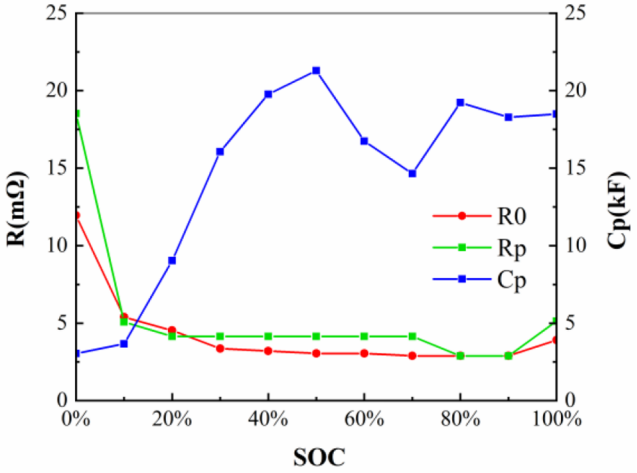

Figure 6. Parameters of every single cell's SOC points.

2.3. Series−Parallel Battery Pack Model. The cell's maximum possible capacity C_{max}, the single cell's operating current I, and the single cell's initial SOC are utilized as model input parameters in the single cell simulation model, which is built in Simulink. The SOC of the single cell's present state is calculated using the ampere-hour integration technique, and the R_0, R_p, and C_p values under various single cell SOC points are calculated using the interpolation method.

2.3.1. Parallel-Connected Battery Pack Model. The Thevenin model of two parallel-connected individual cells is shown in Figure 7. Each branch of the parallel-connected

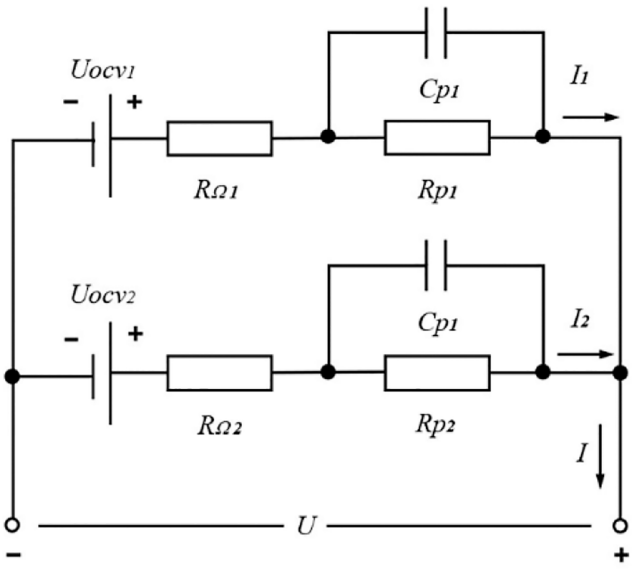

Figure 7. Thevenin model of two parallel-connected individual cells.

battery pack has the same voltage, and the sum of branch current equals the total current. The trunk current is I, and the branch currents are I_1 and I_2. According to Kirchhoff's current law, the formula is

$$V = U_{OCV1} - U_{p1} - I_1 R_{\Omega 1} \quad (4)$$

$$V = U_{OCV2} - U_{p2} - I_2 R_{\Omega 2} \quad (5)$$

$$I_1 R_{\Omega 1} - I_2 R_{\Omega 2} = U_{OCV1} - U_{p1} - U_{OCV2} + U_{p2} \quad (6)$$

$$I = I_1 + I_2 \quad (7)$$

In the same way, the $k \times k$ matrix expression is obtained after sorting out the branch current calculation equation:

$$\begin{bmatrix} R_{\Omega 1} - R_{\Omega 2} & 0 & 0 & 0 \\ 0 & R_{\Omega 2} - R_{\Omega 3} & 0 & 0 \\ 0 & 0 & \ddots & 0 \\ 0 & 0 & \cdots & R_{\Omega(k-1)} - R_{\Omega k} \\ 1 & 1 & \cdots & 1 \quad 1 \end{bmatrix} \begin{bmatrix} I_1 \\ I_2 \\ \vdots \\ I_{k-1} \\ I_k \end{bmatrix} = \begin{bmatrix} U_{OCV1} - U_{p1} - U_{OCV2} + U_{p2} \\ U_{OCV2} - U_{p2} - U_{OCV3} + U_{p3} \\ \vdots \\ U_{OCV(k-1)} - U_{p(k-1)} - U_{OCVk} + U_{pk} \\ I \end{bmatrix} \quad (8)$$

where I_k is the current of the kth branch, U_{OCVk} is the open-circuit voltage of the kth single cell, $R_{\Omega k}$ is the Ohmic resistance of the kth single cell, U_{pk} is the polarization voltage of the kth single cell.

https://doi.org/10.1021/acsomega.3c00266
ACS Omega 2023, 8, 10512−10524

$$U_{pk} = I_k R_{pk}(1 - e^{-t/R_{pk}C_{pk}}) \quad (9)$$

2.3.2. Series-Connected Battery Pack Model. The "barrel effect" shows that the series-connected battery pack's available capacity depends on the series-connected battery pack with the smallest available charging capacity and available discharge capacity in the series−parallel battery pack. If the number of the series-connected batteries is n, the group capacity and SOC are denoted as C_{nS} and SOC_{nS}. C_{nS} and SOC_{nS} can be expressed as

$$C_{nS} = \min[C_1 \times \mathrm{SOC}_1, C_2 \times \mathrm{SOC}_2 \cdots C_n \times \mathrm{SOC}_n] + \min[C_1 \times (1 - \mathrm{SOC}_1), C_2 \times (1 - \mathrm{SOC}_2) \cdots C_n \times (1 - \mathrm{SOC}_n)] \quad (10)$$

$$\mathrm{SOC}_{nS} = \frac{\min[C_1 \times \mathrm{SOC}_1, C_2 \times \mathrm{SOC}_2 \cdots C_n \times \mathrm{SOC}_n]}{C_{nS}} \quad (11)$$

The total voltage of the series−parallel battery pack equals the sum of each parallel battery pack voltage. $U_{\mathrm{OCV}kS}$ can be expressed as

$$U_{\mathrm{OCV}kS} = \sum_{k=1}^{n} U_{\mathrm{OCV}k} \quad (12)$$

2.3.3. 2P3S Battery Pack Model. The topological map of the 2P3S (the 2P3S battery pack consists of three parallel-connected battery packs in series, and the parallel-connected battery pack consists of two individual cells) battery pack model is shown in Figure 8. The 2P3S battery pack's capacity

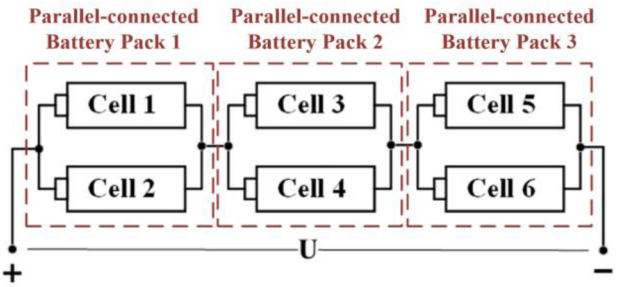

Figure 8. Topological map of the 2P3S battery pack model.

is C_{2P3S}, and the 2P3S battery pack's SOC is SOC_{2P3S}. C_{2P3S} and SOC_{2P3S} can be expressed as

$$C_{2P3S} = \min[C_{Par1} \times \mathrm{SOC}_{Par1}, C_{Par2} \times \mathrm{SOC}_{Par2}, C_{Par3} \times \mathrm{SOC}_{Par3}] + \min[C_{Par1} \times (1 - \mathrm{SOC}_{Par1}), C_{Par2} \times (1 - \mathrm{SOC}_{Par2}), C_{Par3} \times (1 - \mathrm{SOC}_{Par3})] \quad (13)$$

$$\mathrm{SOC}_{2P3S} = \frac{\min[C_{Par1} \times \mathrm{SOC}_{Par1}, C_{Par2} \times \mathrm{SOC}_{Par2}, C_{Par3} \times \mathrm{SOC}_{Par3}]}{C_{2P3S}} \quad (14)$$

To decouple the calculation of a single cell, the current of a single cell in the battery pack is the same, and the sum of all single-cell parameters is the parameter of the battery pack, such as the battery pack's total voltage U, polarization voltage U_p, output power P, etc.

2.3.4. Battery Model Validation. A constant-temperature and -humidity room, as well as a battery test platform, may be used to test the 2P3S battery pack at 11.1 V, 4 Ah once the model has been constructed. The comparison curve between the measured and simulated terminal voltages of the battery pack under the condition of constant current charge and discharge is shown in Figure 9. The highest discrepancy between the simulated value and the measured value is less than 5%, showing that the developed series−parallel battery pack simulation model may be utilized to investigate different combinations of battery module types.

3. INFLUENCE OF INDIVIDUAL CELL PARAMETER DIFFERENCE ON BATTERY PACK PERFORMANCE

To avoid the impact of different battery parameters on the capacity utilization, energy utilization, and terminal voltage of the battery pack, the individual cells are typically classified consistently in engineering, and then the individual cells with similar performance parameters are picked to produce a battery pack in series−parallel to fulfill the criteria and characteristics of the electric vehicle's power system. However, Baumhöfer et al. evaluated 48 individual cells in the same batch under the same conditions. After individual cells are charged and discharged for 1000 cycles, the difference in capacity characteristics between individual cells will still increase to 10%.[9] It is difficult to avoid the phenomenon of individual cell parameter difference. The influence of Ohmic resistance difference, polarization difference, and capacity difference of individual cells on capacity utilization, energy utilization, and terminal voltage after battery grouping is explored by the measurement of individual cell parameter difference.

3.1. Influence of Cell Parameter Difference on the Performance of the Series-Connected Battery Pack. *3.1.1. Theoretical Analysis of Individual Cell Parameter Difference of Series-Connected Battery Pack.* The common parameter differences among individual cells in series-connected battery packs include Ohmic resistance difference, polarization difference, and capacity difference. The impact of these three characteristics on the performance of the series-connected battery pack is investigated using the established battery module model. The polarization difference was simplified as the polarization internal resistance difference.

The topological map of Cell 1, Cell 2, Cell 3, and Cell 4 is shown in Figure 10. $R_{\Omega i}$ is Cell i's Ohmic resistance. Ci is Cell i's capacity. U_{pi} is single Cell i's polarization voltage. V_i is single Cell i's terminal voltage.

3.1.1.1. Different Ohmic Resistance between Individual Cells. Suppose $R_{\Omega 1} < R_{\Omega 2}$, $C_1 = C_2 = C$, and other state parameters of Cell 1 and Cell 2 are the same. Cell 1 and Cell 2 initial SOCs are 100%. Combining eqs 2 and 3 can give the battery's capacity utilization.

The battery's capacity utilization can be expressed as

$$\eta_C = \frac{(1 - \mathrm{SOC}|_{\mathrm{cutoff}}) \times C}{C} = 1 - \mathrm{SOC}|_{\mathrm{cutoff}} \quad (15)$$

According to the principle that cells are connected in series, the capacity remains constant, combining eqs 2, 3, and 15 can give the series-connected battery pack's capacity utilization.

$$\eta_C = 1 - f^{-1}(U_{\mathrm{OCV}} + IR_{\Omega 2} - IR_{\Omega 1}) \quad (16)$$

t_1 the is single Cell 1's usage time from discharge to cutoff voltage, and t_2 is single Cell 2's using time from discharge to

https://doi.org/10.1021/acsomega.3c00266
ACS Omega 2023, 8, 10512−10524

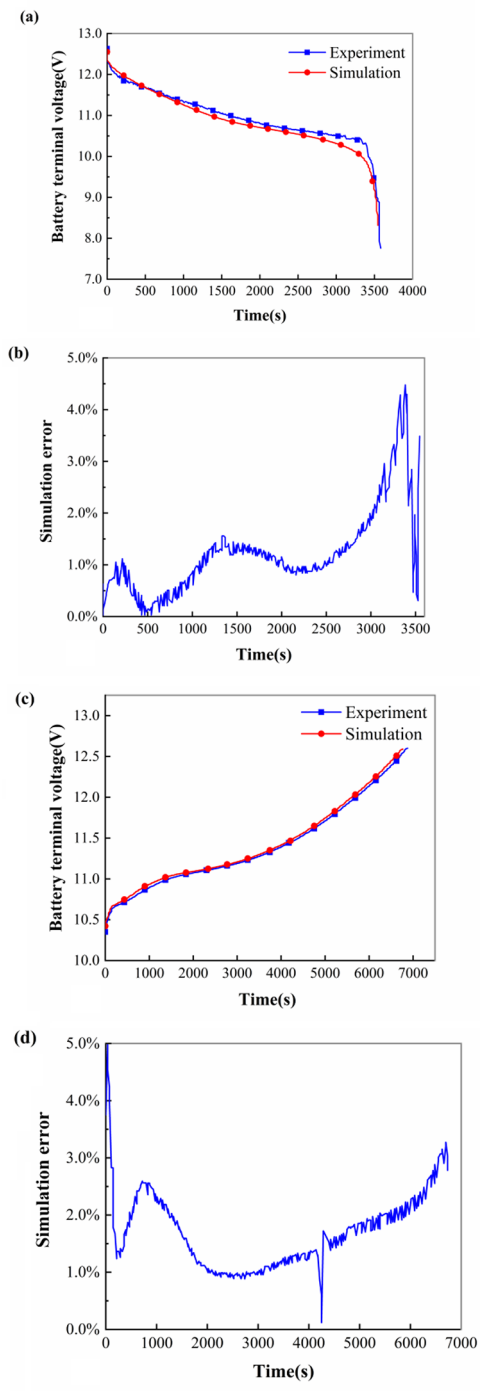

Figure 9. Comparison curve between the measured and simulated terminal voltages of the battery pack under the condition of constant current charge and discharge: (a) battery terminal voltage under constant current discharge condition; (b) discrepancy between the experiment and simulation; (c) battery terminal voltage under constant current charge condition; (d) discrepancy between the experiment and simulation.

cutoff voltage. The energy utilization of a battery is the ratio of discharge energy to charging energy. The energy utilization of the series-connected battery pack by Cell 1 and Cell 2 can be expressed as

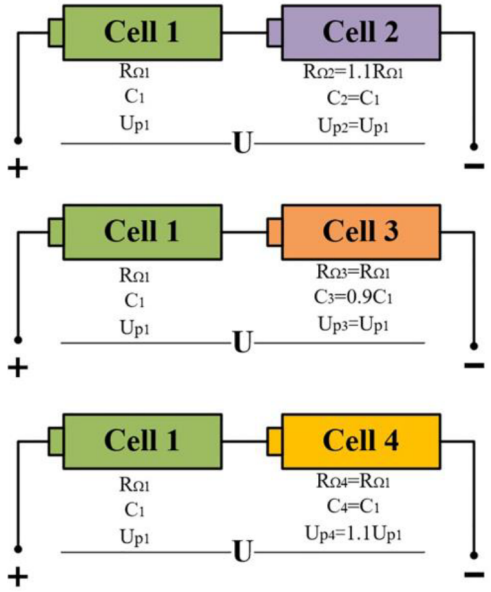

Figure 10. Topological map of Cell 1/Cell 2/Cell 3/Cell 4.

$$\eta_E = \frac{\int_0^{t_2} [V_2(t) + V_1(t)]\, dt}{2\int_0^{t_1} V_1(t)\, dt} \tag{17}$$

3.1.1.2. Different Capacity between Individual Cells. Suppose $C_1 < C_3$ and other state parameters of single Cell 1 and single Cell 3 are the same. Single Cell 1 and single Cell 3 initial SOCs are 100%. Combining eqs 2 and 3 can give the battery's OCV.

$$U_{OCV} = f\left(1 - \frac{It}{C}\right) \tag{18}$$

Since $C_1 < C_3$, it can be seen from eqs 1 and 18 that $V_1 < V_3$. t_3 is single Cell 3's usage time from discharge to cutoff voltage. The capacity utilization of the series-connected battery pack by Cell 1 and Cell 3 can be expressed as eq 19. The energy utilization of the series-connected battery pack by Cell 1 and Cell 3 can be expressed as eq 20.

$$\eta_C = \frac{C_1}{C_3} \tag{19}$$

$$\eta_E = \frac{\int_0^{t_3} [V_3(t) + V_1(t)]\, dt}{2\int_0^{t_1} V_1(t)\, dt} \tag{20}$$

3.1.1.3. Different Degrees of Polarization between Individual Cells. Suppose $U_{p1} < U_{p4}$ and other state parameters of Cell 1 and Cell 4 are the same. Cell 1 and Cell 4 initial SOCs are 100%. Combining eqs 2 and 3 can give $V_1 > V_4$. t_4 is single Cell 4's usage time from discharge to cutoff voltage. The capacity utilization of the series-connected battery pack by Cell 1 and Cell 4 can be expressed as eq 21. The energy utilization of the series-connected battery pack by Cell 1 and Cell 4 can be expressed as eq 22.

$$\eta_C = 1 - f^{-1}(U_{OCV} + IR_{p4} - IR_{p1}) \tag{21}$$

https://doi.org/10.1021/acsomega.3c00266
ACS Omega 2023, 8, 10512−10524

$$\eta_E = \frac{\int_0^{t_4} [V_4(t) + V_1(t)]\, dt}{2\int_0^{t_1} V_1(t)\, dt} \quad (22)$$

The capacity utilization and energy utilization are used to evaluate the battery pack's performance based on the above derivation results. When there is an Ohmic resistance difference between the individual cells, the individual cells with the highest Ohmic resistance limit the series-connected battery pack's performance. When there is a capacity difference between individual cells, the battery pack's performance is determined by the individual cells with the smallest capacity. When there is a polarization difference between individual cells, the battery pack's performance is determined by the single cell with the largest polarization degree.

3.1.2. Simulation Analysis of Parameter Difference of Individual Cells in Series-Connected Battery Pack. Based on the designed series−parallel battery module model, the impact of Ohmic resistance difference, capacity difference, and polarization difference between individual cells on the performance of the series-connected battery pack is simulated and analyzed. The single Cell 1 was compared with Cell 2/Cell 3/Cell 4 in series. With single Cell 1 as the reference and all other parameters of single Cell 1 held constant, the Ohmic resistance of single Cell 2 was 10% higher than that of single Cell 1, the capacity of single Cell 3 was 10% lower than that of single Cell 1, and the polarization resistance of single Cell 4 was 10% higher than that of single Cell 1. The four individual cells' initial SOC was set to 100%. The four individual cells' discharge conditions were set to a constant current of 0.5C rate and 2C rate. The capacity utilization and energy utilization of the battery pack at a constant current discharge of 0.5C/2C rate when Cell 1 and Cell 2/Cell 3/Cell 4 are in series as shown in Tables 3 and 4.

Table 3. Simulation Results at a Constant Current Discharge Rate of 0.5C in Series

cells	discharge time/s	capacity utilization/%	energy utilization/%
Cell 1−Cell 1	7188	100.00	100.00
Cell 1−Cell 2	6872	96.58	95.07
Cell 1−Cell 3	6491	90.00	90.30
Cell 1−Cell 4	7161	99.68	99.62

Table 4. Simulation Results at a Constant Current Discharge Rate of 2C in Series

cells	discharge time/s	capacity utilization/%	energy utilization/%
Cell 1−Cell 1	1721	100.00	92.12
Cell 1−Cell 2	1533	89.77	82.03
Cell 1−Cell 3	1421	84.21	76.81
Cell 1−Cell 4	1683	95.85	90.22

Tables 3 and 4 show that, when the individual cells are connected in series, the individual cells' capacity difference has the greatest impact on the individual cells' capacity utilization and individual cells' energy utilization, while the Ohmic internal resistance and polarization difference of the individual cells have a limited impact on the individual cells' capacity utilization and individual cells' energy utilization. From a comparison of Tables 3 and 4, it can be seen that, under different discharge rates, the influence of monomer battery capacity difference on Cell 1 > Cell 4 > Cell 2 > Cell 3 is the same trend. However, the influence of internal resistance and polarization effect of monomer battery on capacity utilization and energy utilization of a monomer battery gradually increases with the increase of current.

In addition to individual cells' capacity utilization and individual cells' energy utilization, individual cells' terminal voltage is also an important indicator of the battery pack's performance. The operating condition is set to discharge the single cell at a 1C rate and reaches the single cell's discharge cutoff voltage. The four individual cells' initial SOC is 100%. The simulation results of four individual cells during constant current discharge are shown in Figure 11.

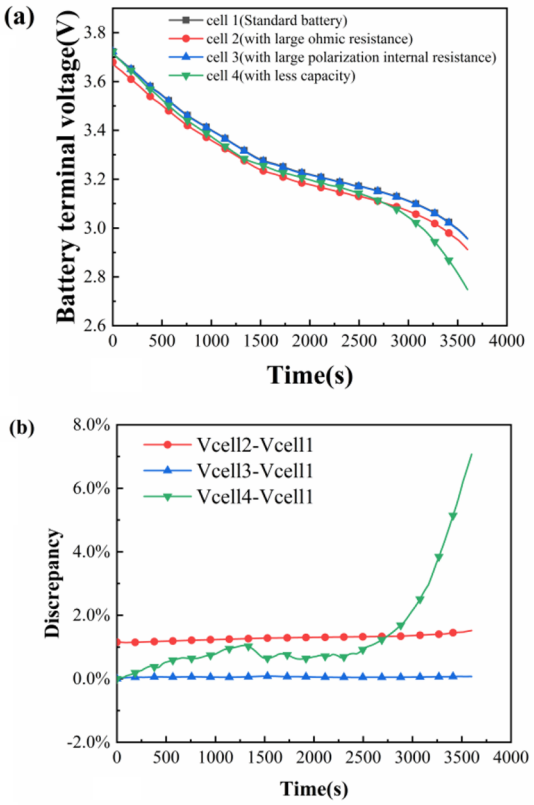

Figure 11. Simulation results of every single cell during constant current discharge: (a) OCV curve of 4 individual cells during constant current discharge; (b) discrepancy between VCell 1−VCell 2/VCell 3/VCell 4.

From Figure 11, compared with Cell 1, Cell 2 reaches the discharge cutoff voltage first under the constant current discharge condition. Moreover, the terminal voltage of Cell 2 with larger Ohmic internal resistance is lower than that of Cell 1 under the whole constant current discharge condition. The difference between the terminal voltage of Cell 2 and Cell 1 is proportional to the Ohmic internal resistance. Therefore, the discharge amount of the series battery pack depends on Cell 2, and the Ohmic internal resistance can affect the discharge energy and discharge power of the battery pack at the same time.

The individual cells' polarization resistance difference has little impact on the individual cells' terminal voltage. There are two main causes behind this. First, the polarization effect of the battery has a weak effect on the battery under constant current

https://doi.org/10.1021/acsomega.3c00266
ACS Omega 2023, 8, 10512−10524

conditions, and second, the polarization resistance is smaller than the Ohmic resistance.

The influence of the battery capacity difference on the battery terminal voltage is gradually increasing, because the battery capacity, the SOC, and the OCV of the battery are also different in the actual situation, which leads to the difference in the battery terminal voltage. However, the SOC starting value of the simulation model is the same, so the terminal voltage difference increases with the increase of the SOC difference.

When the energy utilization rate and capacity utilization rate are used as evaluation indexes to evaluate the performance of series battery pack, the capacity difference between individual cells has the greatest influence on the available energy value of the series battery pack. When the terminal voltage is used as an evaluation index to evaluate the power performance of the series battery pack, the difference of Ohmic internal resistance has little effect on the performance, but the effect will increase with the increase of current. The polarization difference has little effect under stable discharge conditions, and the effect of capacity difference on the performance of the battery pack will increase with the increase of the discharge depth of the battery.

3.2. Influence of Internal Resistance Difference of Single Cell on Parallel-Connected Battery Pack Performance. The individual cells' SOC difference of each branch of the parallel-connected battery pack is not stable, and variations in standing and drastic working conditions will result in the disappearance of individual cells' SOC difference, which has little significance. The capacity difference of the individual cells is frequently not a single variable. The reason for the individual cells' capacity change may be the individual cells' temperature change, the individual cells' aging with the increase of cycle times, or the damage caused by overcharging and overdischarging to the individual cells. Because the aforementioned changes are frequently accompanied by the changes in polarization capacitance, polarization resistance, and Ohmic resistance of individual cells, studying the capacity difference alone is of limited value. Because the battery module is made up of a single battery connected in series, and the single battery is made up of a single cell connected in parallel, the impact of the capacity difference of every single cell in a single battery is investigated. Because of the parameter difference of individual cells, single batteries' capacity might fluctuate substantially in the early stages. As a result, the impact of the individual cells' internal resistance differential on the performance of the parallel-connected battery pack is investigated using the designed parallel-connected battery model.

The Ohmic resistance of single Cell 5 is 10% larger than that of single Cell 6, and the capacity and initial SOC of are single Cell 5 and single Cell 6 are the same. The topological map of single Cell 5 and single Cell 6 is shown in Figure 12. The capacity utilization and energy utilization of single Cell 5 and single Cell 6 at a constant current discharge of 1C rate in parallel are shown in Table 5.

The individual cells' operating conditions are set to a constant current discharge of 1C rate. The simulation results of the current of Cell 5 and Cell 6 and the terminal voltage of the parallel-connected battery pack are shown in Figure 13a. The SOC variation curves of Cell 5 and Cell 6 are shown in Figure 13b.

According to the parameter identification results obtained by the HPPC experiment, the Ohmic internal resistance and polarization internal resistance of individual cells fluctuate greatly at the end of charge and discharge; that is, when the single cell's SOC is greater than 90% or less than 10%, the Ohmic internal resistance and polarization internal resistance of individual cells increase significantly at the end of charge

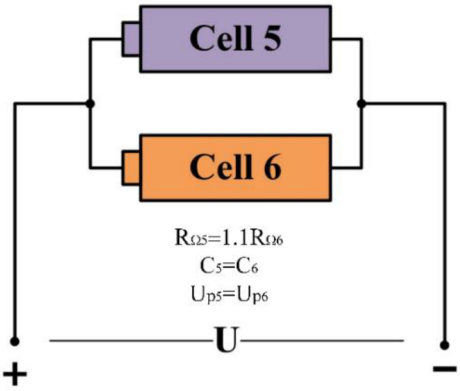

Figure 12. Topological map of Cell 5 and Cell 6.

Table 5. Simulation Results at a Constant Current Discharge Rate of 1C in Parallel

single cell	discharge time/s	capacity utilization/%	energy utilization/%
Cell 5	3413	98.25	100.00
Cell 6	3413	93.40	94.97

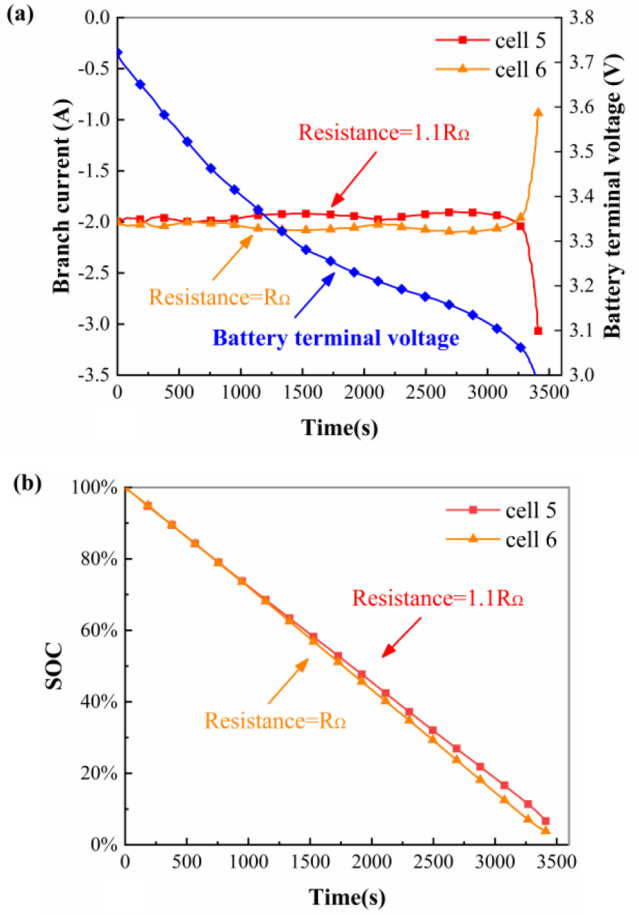

Figure 13. Simulation results for lithium-ion battery parameters in parallel: (a) the single cell current and the parallel-connected battery pack's terminal voltage; (b) SOC curves of Cell 5 and Cell 6.

https://doi.org/10.1021/acsomega.3c00266
ACS Omega 2023, 8, 10512−10524

and discharge. When the single cell's SOC is in the range of 10−90%, the Ohmic internal resistance and polarization internal resistance of individual cells change little. As shown in Figure 13a, the initial discharge current of single Cell 6 is larger than that of single Cell 5 because the initial Ohmic resistance of single Cell 6 is small. When the SOCs of Cell 5 and Cell 6 are the same, the battery terminal voltages of Cell 5 and Cell 6 are the same, and the Ohmic resistance voltage drop of the single Cell 6 will increase. To keep consistent with the battery terminal voltage of single Cell 5, the current of single Cell 6 will increase. However, the SOC decreases rapidly after the current rise, resulting in a rapid decline in open-circuit voltage, which leads to the decrease of the branch current, and the decrease of the current leads to the decrease of the pressure drop caused by the Ohmic resistance, which forms negative feedback during the discharge process and maintains the relative stability of the current distribution. At the end of discharge, the Ohmic internal resistance and polarization effect increased significantly, and the decrease of battery terminal voltage accelerated. The power of single Cell 6 was nearly depleted, and the current output ability was weakened, resulting in a sharp decrease in the current. The current of single Cell 5 increased sharply, and the discharge stopped. As shown in Figure 13b, SOC of single Cell 6 is always lower than that of single Cell 5, and the gap is gradually increasing because the current of single Cell 6 is always higher than that of single Cell 5 before the end of discharge.

The simulation results show that when the internal resistance of the single cell in the parallel battery group is different, the current of the single cell with smaller internal resistance is larger before the end of the discharge, and the current will fluctuate slightly, but it will be balanced by the negative feedback between the individual cells. At the end of the discharge, the Ohmic resistance of the battery increases, and the polarization resistance increases sharply due to the low SOC of the single cell with small internal resistance, resulting in the sudden increase in the current of another single cell.

3.3. Effect of Aging Lithium-Ion Battery on the Performance of Series−Parallel Battery Pack. The number of retired lithium-ion batteries is growing rapidly in tandem with the continued increase in new vehicle sales and ownership of new energy vehicles. However, because the retired battery capacity is 70−80% of the rated capacity, it can still be employed in energy storage systems. Wang et al. has studied the change of the identification parameters when the capacity of the equivalent circuit model decayed to 80% of the initial capacity; that is, the capacity of the aged single cell decreased to 80% of the original, and the internal resistance increased to 166.4% of the initial value.[36]

A 5P2S battery pack model A with an aging single cell is built using the created series−parallel model, and a regular 5P2S battery pack model B is used as a comparison. The topology is shown in Figure 14. Cell 1 is a simulated aging single cell, its capacity is 80% of other cells in the 5P2S battery pack, and the other parameters are the same as those of the other cells in the 5P2S battery pack. The initial full power is utilized, and the operating state is set to a constant current discharge of 1C rate. The discharge ceases when the SOC of any single battery in the battery pack reaches zero. The simulation results are shown in Figure 15.

Figure 15a compares the terminal voltage between the battery pack model A and the battery pack model B in the discharge process. It can be observed from the battery's

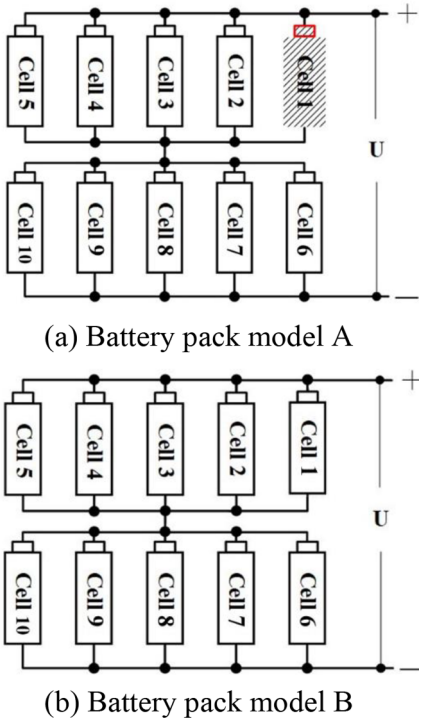

Figure 14. Topological structure of 5P2S battery pack models A and B.

terminal voltage difference curve that the terminal voltage difference between the two battery pack models before the discharge is minor. The SOC of battery pack model A first reaches zero to trigger the simulation stop condition. At this time, the battery pack model A's polarization resistance and Ohmic resistance increase, and the terminal voltage of the battery pack model A decreases, where the aging single cell is placed.

Figure 15b shows the SOC variations of Cell 1, Cell 2, and Cell 6 during constant current discharge. The current flowing through the single battery with the aging single cell in series is identical with that of the conventional single battery. The total capacity of a single battery is equivalent to the sum of every single cell's capacities. As a result of the aging single cell's low capacity, the capacity of the parallel-connected battery pack with the aging single cell is lower than the capacity of the parallel-connected battery pack without the aging single cell. The SOC of the parallel-connected battery pack with the aging single cell declines more quickly than the SOC of the parallel-connected battery pack without the aging single cell. The SOC of an aging single cell declines more quickly those of than other individual cells of the same parallel-connected battery pack.

3.4. Optimization Analysis of Battery Series−Parallel Grouping. Through the above analysis, the capacity of every single cell in the series−parallel battery pack is different, which causes the single cell to overcharge and overdischarge during the charge and discharge cycle, accelerating the aging of the single cell and causing the battery pack's parameter difference to deteriorate. The battery pack's "barrel effect" is likewise steadily exacerbated, reducing the battery pack's usable capacity significantly. The aging single cell will affect the parallel-connected individual cells in the same battery pack, eventually resulting in the battery pack's cycle life being

https://doi.org/10.1021/acsomega.3c00266
ACS Omega 2023, 8, 10512−10524

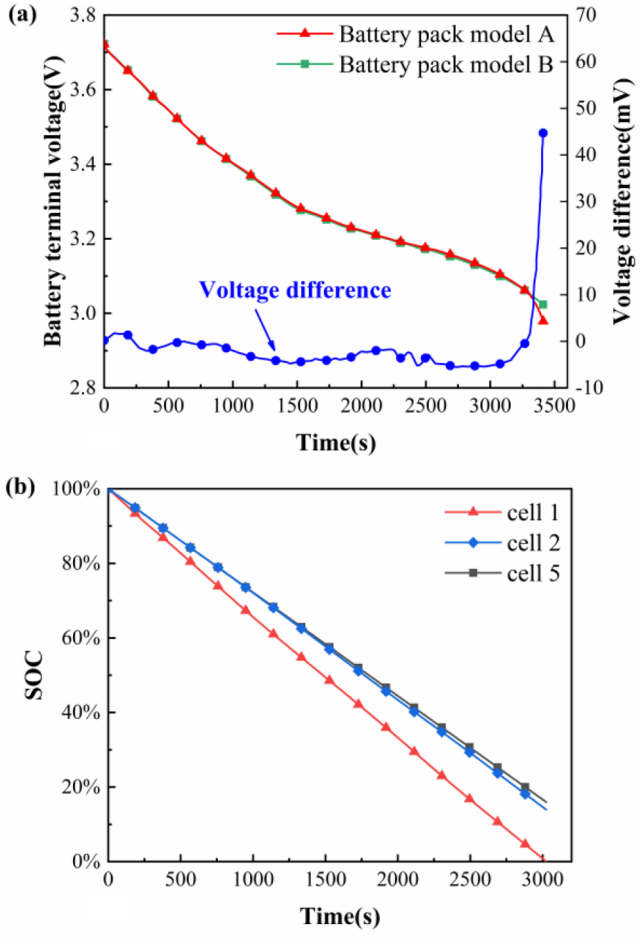

Figure 15. Simulation results of individual cells during constant current discharge: (a) battery terminal voltage curve of Cell 1 and Cell 5 during constant current discharge; (b) SOC curves of 3 individual cells during constant current discharge.

terminated. Based on the study of simulation results, the following optimization suggestions are made to reduce the influence of single-cell parameters difference on battery performance.

3.4.1. Individual Cell Battery Series into the Battery Pack. For series-connected battery packs, the capacity difference of a single battery has the biggest influence on series-connected battery pack performance. The series−parallel battery pack consists of parallel-connected battery packs in series, and a parallel-connected battery pack consists of individual cells in parallel. Thus, the weight of capacity difference should be enhanced in parallel-connected battery pack parameter selection. At the same time, the balancing function of the battery management system may adjust the capacity of parallel-connected battery packs, allowing the single cell with the smallest capacity to be fully charged and discharged while avoiding inconsistencies in battery pack characteristics.

3.4.2. Individual Cell Battery Parallel into the Battery Pack. For a parallel-connected battery pack, the negative feedback formed by the coupling of parameters between individual cells can keep the current stable before the end of charge and discharge. However, the current instability caused by the sudden increase of Ohmic resistance and polarization resistance before the end of charge and discharge must be suppressed. It is possible to test the Ohmic resistance and polarization resistance of a single cell in a group. When the Ohmic resistance of some individual cells is too high, the single cell with the strongest polarization effect and the highest polarization resistance at the end of charge and discharge can be chosen to suppress the current change caused by the polarization voltage mutation of the single cell with the lowest internal resistance at the end of charge and discharge.

3.4.3. Problem of Accelerated Aging of Aging Individual Cells in Battery Packs. To address the issue of accelerated aging of aging individual cells caused by a parameter difference in series−parallel battery packs, the voltage change curve at the end of charge and discharge of a parallel-connected battery pack in various aging stages must be examined. The charging and discharging cutoff voltage of the single battery where the aging single cell is located is adjusted to avoid further deterioration of overcharge and overdischarge of the aging single cell, and the voltage characteristic curve recognition algorithm of an aging single cell is established to provide early warning in time.

4. CONCLUSIONS

The Thevenin equivalent circuit model of a single cell is built based on Simulink. On this foundation, a model of a series−parallel battery pack in MATLAB/Simulink is developed, and the impact of various individual cell characteristics on the performance of the battery pack in series and parallel is investigated, providing a reference for the weight of single-cell screening parameters when the battery is assembled. The impact of an aging single cell on a battery pack's performance was investigated, and the notion of evaluating battery individual cell aging by monitoring the terminal voltage change rate of individual cells at the end of charge and discharge was offered. The following conclusions were reached based on the preceding simulation study of the group optimization idea of a single cell when battery packs connected in series and parallel are analyzed.

(1) When cells are connected in series, the capacity difference of a single cell affects the battery pack's energy index, and the capacity and Ohmic resistance differences of cells affect the battery pack's power index.

(2) When cells are connected in parallel, the difference in Ohmic resistance between the individual cells causes a branch current imbalance, the energy utilization of some individual cells is low, and the individual cells' unbalanced current expands sharply at the end of discharge, causing individual cells' overdischarge and battery life to be shortened.

(3) Interestingly, we found that when there is an aging single cell in a series−parallel battery pack, the terminal voltage of the single battery module containing the aging single cell will decrease sharply at the end of discharge. By evaluating the change rate of battery terminal voltage at the end of discharge, it can be used as a method to evaluate the aging degree of single battery module. The research results provide a reference for connecting batteries into battery packs, in particular, the screening of retired power battery packs and the way to reconnect them into battery packs.

https://doi.org/10.1021/acsomega.3c00266
ACS Omega 2023, 8, 10512−10524

AUTHOR INFORMATION

Corresponding Authors

Yong Cheng − *School of Energy and Power Engineering, Shandong University, Jinan 250061, People's Republic of China*; orcid.org/0000-0002-5126-4255; Email: cysgd@sdu.edu.cn

Wei Yin − *School of Energy and Power Engineering, Shandong University, Jinan 250061, People's Republic of China*; Email: yinwei999@sdu.edu.cn

Authors

Yongqi Wang − *School of Energy and Power Engineering, Shandong University, Jinan 250061, People's Republic of China*

Yujie Zhao − *School of Energy and Power Engineering, Shandong University, Jinan 250061, People's Republic of China*

Siyuan Zhou − *Yabtai Port Hlodings Co., Ltd. Port Ore Terminal Branch, Yantai 264000, People's Republic of China*

Qingzhong Yan − *Ruinuo (Jinan) Power Technology Co., Ltd, Jinan 250118, People's Republic of China*

Han Zhan − *School of Energy and Power Engineering, Shandong University, Jinan 250061, People's Republic of China*

Complete contact information is available at: https://pubs.acs.org/10.1021/acsomega.3c00266

Author Contributions

Y.W.: software, formal analysis, methodology, visualization, writing−original draft, review, and editing. Y. Z., H. Z.: software, data curation, validation, visualization, writing−original draft. S.Z., Q.Y., W.Y.: investigation project administration, visualization, Y.C.: funding acquisition, project administration, resources, writing−review and editing.

Notes

The authors declare no competing financial interest.

ACKNOWLEDGMENTS

This work was supported by the Natural Science Foundation of Shandong Province (ZR2019MF037).

REFERENCES

(1) Contestabile, M.; Offer, G. J.; Slade, R.; Jaeger, F.; Thoennes, M. Battery Electric Vehicles, Hydrogen Fuel Cells and Biofuels. Which Will Be the Winner? *Energy Environ. Sci.* **2011**, *4* (10), 3754.

(2) Eberle, D. U.; von Helmolt, D. R. Sustainable Transportation Based on Electric Vehicle Concepts: A Brief Overview. *Energy Environ. Sci.* **2010**, *3* (6), 689.

(3) Wang, Y.; Yin, W.; Yan, Q.; Cheng, Y. Emission Characteristics of Particulate Matter Emitted by Typical Off-Road Construction Machinery. *Environmental Science and Pollution Research* **2022**, *29*, 44220−44232.

(4) Li, Y.; Tang, W.; Abubakar, S.; Wu, G. Construction of a Compact Skeletal Mechanism for Acetone−n−Butanol−Ethanol (ABE)/Diesel Blends Combustion in Engines Using a Decoupling Methodology. *Fuel Process. Technol.* **2020**, *209*, No. 106526.

(5) Li, Y.; Tang, W.; Chen, Y.; Liu, J.; Lee, C. F. Potential of Acetone-Butanol-Ethanol (ABE) as a Biofuel. *Fuel* **2019**, *242*, 673−686.

(6) Baumann, M.; Wildfeuer, L.; Rohr, S.; Lienkamp, M. Parameter Variations within Li-Ion Battery Packs − Theoretical Investigations and Experimental Quantification. *Journal of Energy Storage* **2018**, *18*, 295−307.

(7) Tarascon, J.-M.; Armand, M. Issues and Challenges Facing Rechargeable Lithium Batteries. *Nature* **2001**, *414*, 359−367.

(8) Offer, G. J.; Yufit, V.; Howey, D. A.; Wu, B.; Brandon, N. P. Module Design and Fault Diagnosis in Electric Vehicle Batteries. *J. Power Sources* **2012**, *206*, 383−392.

(9) Baumhöfer, T.; Brühl, M.; Rothgang, S.; Sauer, D. U. Production Caused Variation in Capacity Aging Trend and Correlation to Initial Cell Performance. *J. Power Sources* **2014**, *247*, 332−338.

(10) Kenney, B.; Darcovich, K.; MacNeil, D. D.; Davidson, I. J. Modelling the Impact of Variations in Electrode Manufacturing on Lithium-Ion Battery Modules. *J. Power Sources* **2012**, *213*, 391−401.

(11) Zhang, J.; Ci, S.; Sharif, H.; Alahmad, M. Modeling Discharge Behavior of Multicell Battery. *IEEE Transactions on Energy Conversion* **2010**, *25*, 1133−1141.

(12) Qian, K.; Li, Y.; He, Y.-B.; Liu, D.; Zheng, Y.; Luo, D.; Li, B.; Kang, F. Abuse Tolerance Behavior of Layered Oxide-Based Li-Ion Battery during Overcharge and over-Discharge. *RSC Adv.* **2016**, *6* (80), 76897−76904.

(13) Brand, M. J.; Kolp, E. I.; Berg, P.; Bach, T.; Schmidt, P.; Jossen, A. Electrical Resistances of Soldered Battery Cell Connections. *Journal of Energy Storage* **2017**, *12*, 45−54.

(14) Ouyang, D.; Chen, M.; Liu, J.; Wei, R.; Weng, J.; Wang, J. Investigation of a Commercial Lithium-Ion Battery under Overcharge/over-Discharge Failure Conditions. *RSC Adv.* **2018**, *8* (58), 33414−33424.

(15) Zheng, Y.; Qian, K.; Luo, D.; Li, Y.; Lu, Q.; Li, B.; He, Y.-B.; Wang, X.; Li, J.; Kang, F. Influence of Over-Discharge on the Lifetime and Performance of $LiFePO_4$/Graphite Batteries. *RSC Adv.* **2016**, *6* (36), 30474−30483.

(16) Xiong, R.; Zhang, Y.; He, H.; Zhou, X.; Pecht, M. G. A Double-Scale, Particle-Filtering, Energy State Prediction Algorithm for Lithium-Ion Batteries. *IEEE Transactions on Industrial Electronics* **2018**, *65*, 1526−1538.

(17) Sun, F.; Xiong, R. A Novel Dual-Scale Cell State-of-Charge Estimation Approach for Series-Connected Battery Pack Used in Electric Vehicles. *J. Power Sources* **2015**, *274*, 582−594.

(18) Wen, F.; C. Lin, J. J.; Wang, Z. A New Evaluation Method to the Consistency of Lithium-Ion Batteries in Electric Vehicles. *Asia−Pacific Power And Energy Engineering Conference*, 2012.

(19) Zhang, X.; Wang, Y.; Wu, J.; Chen, Z. A Novel Method for Lithium-Ion Battery State of Energy and State of Power Estimation Based on Multi-Time-Scale Filter. *Applied Energy* **2018**, *216*, 442−451.

(20) Zheng, Y.; Ouyang, M.; Lu, L.; Li, J.; Han, X.; Xu, L.; Ma, H.; Dollmeyer, T. A.; Freyermuth, V. Cell State-of-Charge Inconsistency Estimation for LiFePO4 Battery Pack in Hybrid Electric Vehicles Using Mean-Difference Model. *Applied Energy* **2013**, *111*, 571−580.

(21) Feng, F.; Hu, X.; Liu, K.; Che, Y.; Lin, X.; Jin, G.; Liu, B. A Practical and Comprehensive Evaluation Method for Series-Connected Battery Pack Models. *IEEE Transactions on Transportation Electrification* **2020**, *6*, 391−416.

(22) Duan, B.; Li, Z.; Gu, P.; Zhou, Z.; Zhang, C. Evaluation of Battery Inconsistency Based on Information Entropy. *Journal of Energy Storage* **2018**, *16*, 160−166.

(23) Wang, L.; Wang, L.; Liao, C.; Zhang, W. Research on Multi-Parameter Evaluation of Electric Vehicle Power Battery Consistency Based on Principal Component Analysis. *Journal of Shanghai Jiaotong University (Science)* **2018**, *23*, 711−720.

(24) Jiang, Y.; Jiang, J.; Zhang, C.; Zhang, W.; Gao, Y.; Mi, C. A Copula-Based Battery Pack Consistency Modeling Method and Its Application on the Energy Utilization Efficiency Estimation. *Energy* **2019**, *189*, No. 116219.

(25) Wang, Y.; Cheng, Y.; Xiong, Y.; Yan, Q. Estimation of Battery Open-Circuit Voltage and State of Charge Based on Dynamic Matrix Control - Extended Kalman Filter Algorithm. *Journal of Energy Storage* **2022**, *52*, No. 104860.

(26) Wang, Y.; Yin, W.; Yan, Q.; Cheng, Y. Impact of Sensor Accuracy of Battery Management System on SOC Estimation of Electric Vehicle Based on EKF Algorithm. In *2021 5th CAA*

International Conference on Vehicular Control and Intelligence (CVCI); 2021; pp 1−6. DOI: 10.1109/CVCI54083.2021.9661212.
(27) Rao, R.; Vrudhula, S.; Rakhmatov, D. N. Battery Modeling for Energy Aware System Design. *Computer* **2003**, *36*, 77.
(28) Golubkov, A. W.; Scheikl, S.; Planteu, R.; Voitic, G.; Wiltsche, H.; Stangl, C.; Fauler, G.; Thaler, A.; Hacker, V. Thermal Runaway of Commercial 18650 Li-Ion Batteries with LFP and NCA Cathodes − Impact of State of Charge and Overcharge. *RSC Adv.* **2015**, *5* (70), 57171−57186.
(29) Ahmed, R.; El Sayed, M.; Arasaratnam, I.; Jimi Tjong; Habibi, S. Reduced-Order Electrochemical Model Parameters Identification and SOC Estimation for Healthy and Aged Li-Ion Batteries Part I: Parameterization Model Development for Healthy Batteries. *IEEE J. Emerg. Sel. Topics Power Electron.* **2014**, *2* (3), 659−677.
(30) Hu, X.; Li, S.; Peng, H. A Comparative Study of Equivalent Circuit Models for Li-Ion Batteries. *J. Power Sources* **2012**, *198*, 359−367.
(31) He, H.; Xiong, R.; Fan, J. Evaluation of Lithium-Ion Battery Equivalent Circuit Models for State of Charge Estimation by an Experimental Approach. *Energies* **2011**, *4*, 582−598.
(32) Bizeray, A. M.; Kim, J.-H.; Duncan, S. R.; Howey, D. A. Identifiability and Parameter Estimation of the Single Particle Lithium-Ion Battery Model. *IEEE Transactions on Control Systems Technology* **2019**, *27*, 1862−1877.
(33) Moura, S. J.; Argomedo, F. B.; Klein, R.; Mirtabatabaei, A.; Krstic, M. Battery State Estimation for a Single Particle Model With Electrolyte Dynamics. *IEEE Transactions on Control Systems Technology* **2017**, *25*, 453−468.
(34) Wang, L.; Cheng, Y.; Zou, J. Battery Available Power Prediction of Hybrid Electric Vehicle Based on Improved Dynamic Matrix Control Algorithms. *J. Power Sources* **2014**, *261*, 337−347.
(35) Hu, H.; Xu, X.; Sun, X.; Li, R.; Zhang, Y.; Fu, J. Numerical Study on the Inhibition Control of Lithium-Ion Battery Thermal Runaway. *ACS Omega* **2020**, *5* (29), 18254−18261.
(36) Wang, L.; Cheng, Y.; Zhao, X. A LiFePO4 Battery Pack Capacity Estimation Approach Considering In-Parallel Cell Safety in Electric Vehicles. *Applied Energy* **2015**, *142*, 293−302.

https://doi.org/10.1021/acsomega.3c00266
ACS Omega 2023, 8, 10512−10524